J Fusion Energ (2014) 33:765–769
DOI 10.1007/s10894-014-9746-x

ORIGINAL RESEARCH

Analysis of Power Deposition on Heat Load Components for EAST Neutral Beam Injector

Yongjian Xu · Chundong Hu · Sheng Liu · Ling Yu · NBI Group

Published online: 2 August 2014

Abstract Neutral beam injection is recognized as one of the most effective means of plasma heating. The target values of EAST Neutral beam injector (NBI) are beam energy 50–80 keV, injection beam total power 2–4 MW, beam pulse width 10–100 s. The beam power will deposit on the beam collimator due to the beam divergence and it will cause heat damage to heat load components, or even destroy the entire NBI system. In order to decrease the risk, the beam power deposited on heat load components should be assessed. In this article, the percent of power deposition on each heat load components has been calculated using Gaussian beam transmission model. Comparison of the results measured with water flow calorimeter and calculated results shows the beam transmission model has relative good agreement with real distribution. The results can direct the operation parameter optimization of EAST NBI.

Keywords Neutral beam · Gaussian beam · Heat load components

Introduction

Achievement of the ignition of fusion plasmas is one of the important subjects of plasma heating. It is well known widely that Neutral beam injection (NBI) is the most effective method for effective plasma heating and has been also verified to be applicable for current drive. As the first full superconducting non-circular cross section Tokomak in the world, EAST is used to explore the forefront physics and engineering issues on the construction of Tokomak fusion reactor [1–3]. According to the research plan of the EAST physics experiment, two sets of neutral beam injector will be built and operational in 2014. The target values of EAST NBI are beam energy 50–80 keV, injection beam total power 2–4 MW, beam pulse width 10–100 s [4–8]. The beam power will deposit on the beam collimator due to the beam divergence and it will cause heat damage to heat load components, or even destroy the entire NBI system. In order to decrease the risk, the beam power deposited on heat load components should be assessed. In this article, a Gaussian model has been put forward according to the structure of accelerating grids and beam power density distribution on some key heat load components and collimators is given using the Gauss model [9]. Comparison of the results measured with water flow calorimeter and calculated results shows the beam power density distribution obtained through beam transmission model has relative good agreement with real distribution [10]. It is helpful to direct the operation parameter optimization of EAST NBI.

Principles and Methods

Main components of the NBI system are two high-current ion sources, control system, beam diagnosis system, vacuum system, gas supply system, cooling water system and so on as shown in Fig. 1. The ion source, which is the key device of EAST-NBI, consists of an arc chamber and a beam accelerator. The accelerator of EAST-NBI consists of four-grid electrostatic exaction accelerated systems, which are plasma grid (PG), gradient grid (GG), suppressor grid (SG) and exit grid (EG). Every electrode is composed of

Y. Xu (✉) · C. Hu · S. Liu · L. Yu
Institute of Plasma Physics, Chinese Academy of Sciences, Hefei 230031, China
e-mail: yjxu@ipp.ac.cn

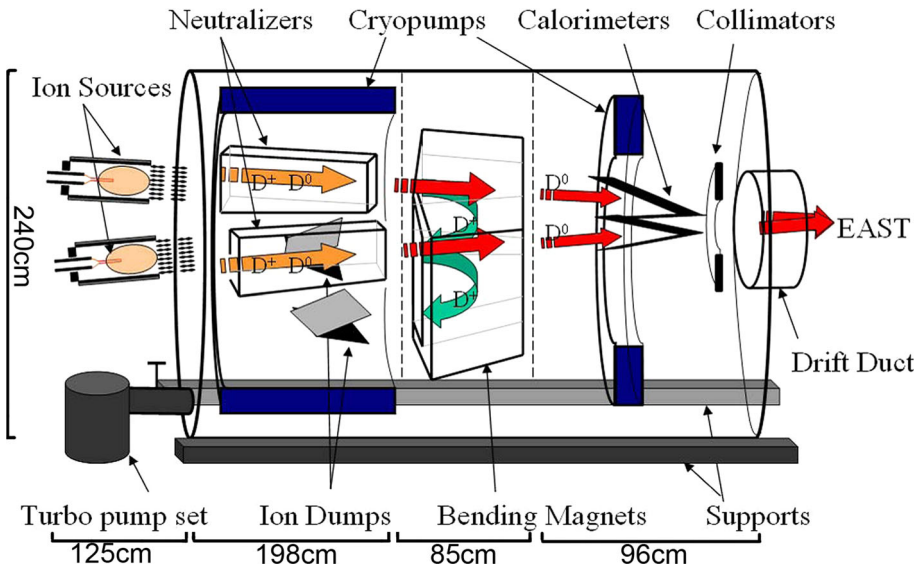

Fig. 1 Schematic view of EAST-NBI

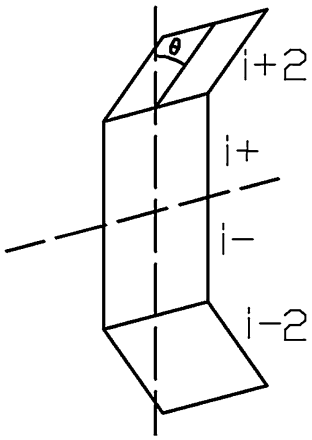

Fig. 2 The assembling schematic diagram of every electrode [θ is the incident angle of beam emitted from the center position of sub-electrode (i + 2, i−2)]

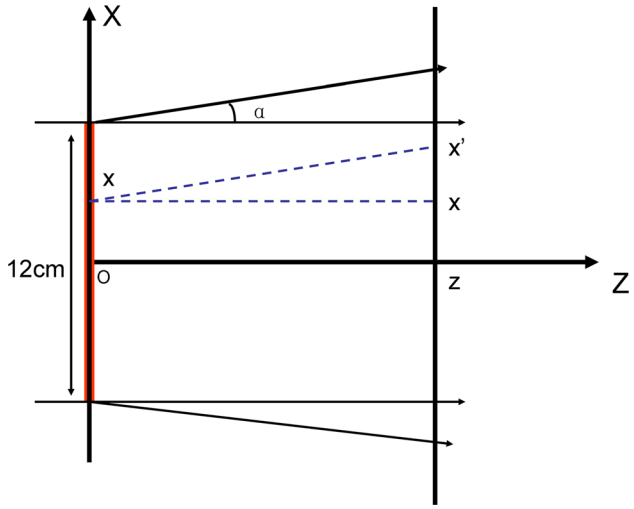

Fig. 3 Geometric relationship of electrodes in X direction (α is the divergence angle in X direction)

four sub-electrodes (i+, i−, i + 2, i−2)and the assembling schematic diagram of every electrode is given by Fig. 2.

EAST neutral beam injector adopts four electrodes electrostatic accelerated extraction system with spatial focusing capability. Every electrode is composed of four sub-electrodes (i+, i−, i + 2, i−2) (See Fig. 2) and the assembling schematic diagram of every electrode is given by Fig. 2.

Figure 2 shows that all sub-electrodes (i+, i + 2, i−, i−2) focus to one point along the beam line. The distribution of beam intensity emitted by arbitrary point source of the electrode in space is

$$I = I_0 \exp\left(-\frac{2r^2}{w^2}\right)$$

where I_0 is the total beam intensity, $w = z^*\tan\varphi$, φ is beam divergence angle. In order to simplify the calculation process, the beam in x or y direction can be considered as the beam emitted from the Gaussian distribution line source with a beam divergence angle.

Calculation of Beam Distribution in X Direction

Not considering the plasma nonuniformity in arc chamber, the beam intensity extracted by all the grids in x direction is the same. Establish a coordinate system as shown in Fig. 3.

As shown in Fig. 3, the beam intensity of x' emitted from point source x in z diagnosis plane is

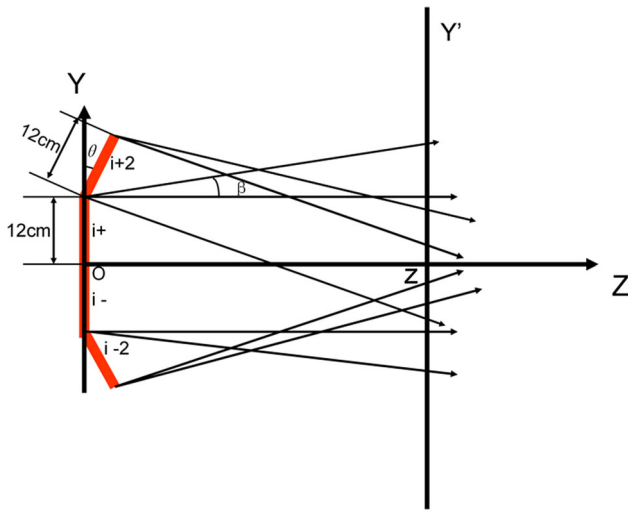

Fig. 4 Geometric relationship of electrodes in Y direction (β is the divergence angle is Y direction)

$$I = I_0 \exp\left[-\frac{2(x' - x)^2}{(z^* \tan\alpha)^2}\right]$$

The beam intensity of x' emitted from x direction electrode is

$$I_{x'} = \int_{-6}^{6} I_0 \exp\left[-\frac{2(x' - x)^2}{(z^* \tan\alpha)^2}\right] dx$$

Using the equation above, the beam intensity of all the points in z diagnosis plane can be obtained.

Calculation of Beam Distribution in Y Direction

As shown in Fig. 4, the beam intensity of y' emitted from point source y in a, b, c and d sub-electrode in z diagnosis plane is listed below

i + 2 sub-electrode

$$I = I_0 \exp\left[-\frac{2(y' - y + z^* \tan\theta)^2}{(z^* \tan\beta)^2}\right]$$

i+ sub-electrode

$$I = I_0 \exp\left[-\frac{2(y' - y)^2}{(z^* \tan\beta)^2}\right]$$

i− sub-electrode

$$I = I_0 \exp\left[-\frac{2(y' - y)^2}{(z^* \tan\beta)^2}\right]$$

i − 2 sub-electrode

$$I = I_0 \exp\left[-\frac{2(y' - y - z^* \tan\theta)^2}{(z^* \tan\beta)^2}\right]$$

the beam intensity of y' point emitted by total electrode can be written

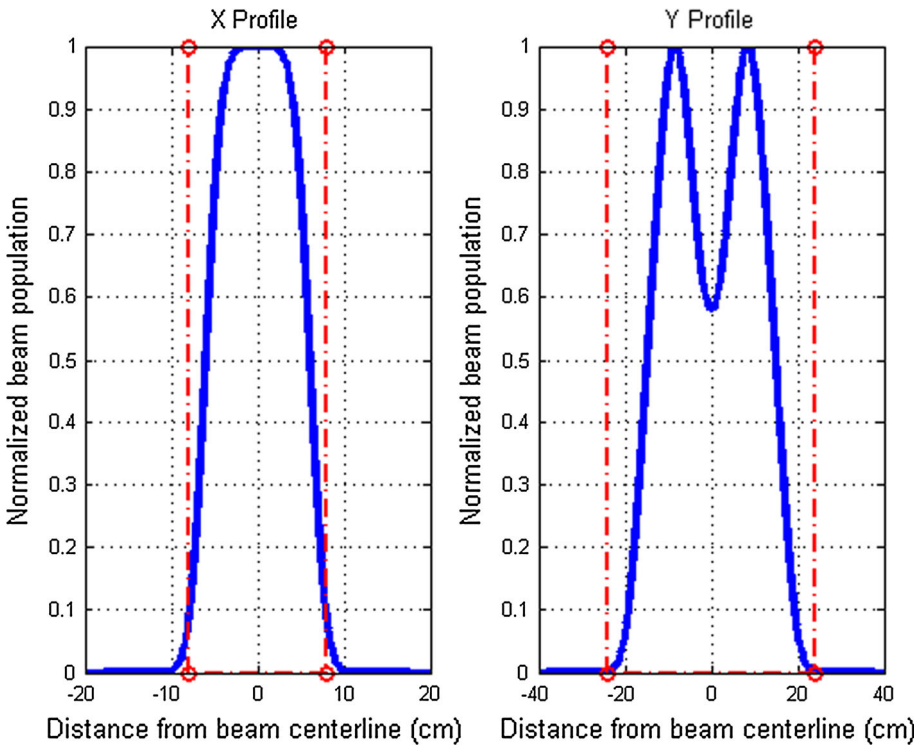

Fig. 5 The beam intensity distribution of collimator of bending magnet ion entrance (z = 274 cm, red dotted line is the border of the beam collimator (16 × 48 cm)) (Color figure online)

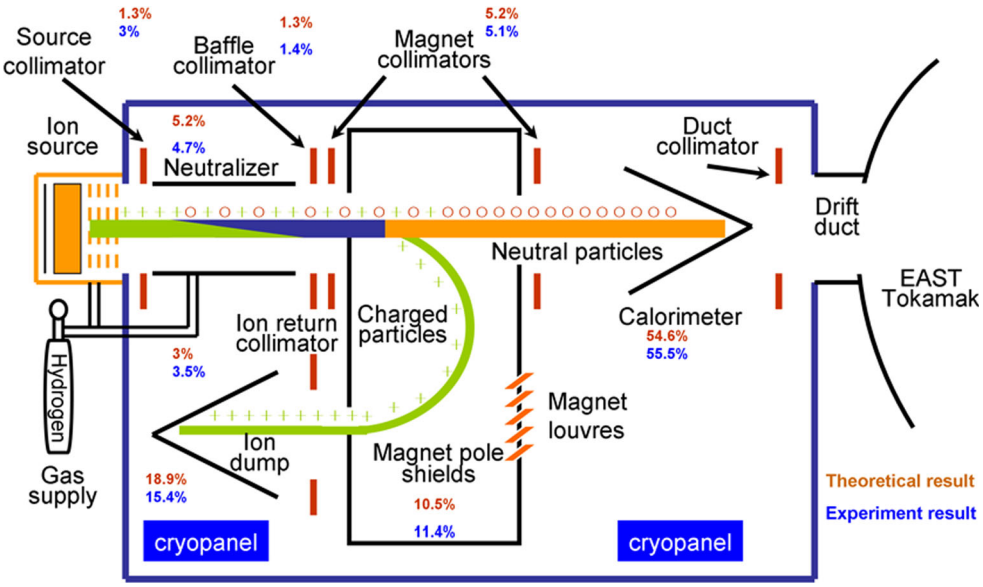

Fig. 6 Beam power deposition distribution on the heat load components (*Orange*: Theoretical results, *Blue*: Experiment results; Vacc = 60 kV) (Color figure online)

$$I_{y'} = \int_{12}^{24} I_0 \exp\left[-\frac{2(y'-y+z^*\tan\theta)^2}{(z^*\tan\beta)^2}\right]dy + \int_{0}^{12} I_0 \exp\left[-\frac{2(y'-y)^2}{(z^*\tan\beta)^2}\right]dy + \int_{-12}^{0} I_0 \exp\left[-\frac{2(y'-y)^2}{(z^*\tan\beta)^2}\right]dy + \int_{-24}^{-12} I_0 \exp\left[-\frac{2(y'-y-z^*\tan\theta)^2}{(z^*\tan\beta)^2}\right]dy$$

Using the equation above, the beam intensity of all the points in z diagnosis plane can be obtained.

Results and Discussions

Take $\theta = 1^\circ\ 5'$, $\alpha = 0.6^\circ$, $\beta = 1.2^\circ$, the beam intensity distribution can be obtained in different key components along beam transmission direction. Figure 5 shows the beam intensity distribution of collimator of bending magnet ion entrance.

Combined with the beam intensity distribution (as shown in Fig. 5), the percent of power deposited on the collimator can be obtained by the method of integrate. Using the same method, the power deposited on the other key heat load components can be obtained. Figure 6 shown the results of percent of power deposited on the key heat load components. Comparing the theoretical results with experiment results, we can find that there are some differences between experiment results and theoretical results for source collimator, magnet pole shields and ion dump. The possible reasons are listed below: (1) as gas flow from the arc chamber and neutralizer, the ion density near the ion source collimator is higher, the collision probability between ion beam and background ion will increase and increasing collision probability will lead to more energy deposition on the source collimator. (2) As the model doesn't consider beam particle species evolution (the beam are considered as 100 % H_1^+ beam), for H_2^+, H_3^+, the orbital radius are different with which of H_1^+, so some beam energy of H_2^+, H_3^+ will deposit on the magnet pole shields and more energy deposit on the magnet pole shield and less energy deposit on the ion dump.

Conclusion

Even though there are some divergences between experiment results and theoretical results, the beam transmission model can direct the operation parameter optimization of EAST NBI.

Acknowledgments This work has been supported by the National Magnetic Confinement Fusion Science Program of China (Grant No. 2013GB101000) and the Presidential Foundation of the Hefei Institutes of Physical Science Chinese Academy of Sciences (Grant No. YZJJ201309).

References

1. Y.X. Wan, Overview of steady state operation of HT-7 and present status of the HT-7U project. Nucl. Fusion **40**, 1057 (2000)
2. J.G. Li, B.N. Wan, Recent progress in RF heating and long-pulse experiments on EAST. Nucl. Fusion **51**, 094007 (2011)
3. B.N. Wan, Recent experiments in the EAST and HT-7 superconducting tokamaks. Nucl. Fusion **49**, 104011 (2011)

4. C.D. Hu, Conceptual design of neutral beam injection system for EAST. Plasma Sci. Technol. **14**, 567 (2012)
5. Y.J. Xu, C.D. Hu, S. Liu, Y.H. Xie, L.Z. Liang, C.C. Jiang, Preliminary experimental study of ion beam extraction of EAST neutral beam injector. Chin. Phys. Lett. **29**, 035201 (2012)
6. C.D. Hu, Preliminary results of ion beam extraction tests on EAST neutral beam injector. Plasma Sci. Technol. **14**, 871 (2012)
7. C.D. Hu, Y.H. Xie, The development of a megawatt-level high current ion source. Plasma Sci. Technol. **14**, 75 (2012)
8. Y.J. Xu, C.D. Hu, Y.L. Xie, J. Li, S. Liu, Y.H. Xie, P. Sheng, Z.M. Liu, L.Z. Liang, Analysis of MW-scale beam extraction of EAST neutral beam injector test-stand. J. Fusion Energ. **32**, 589 (2013)
9. Y.J. Xu, C.D. Hu, Y.L. Xie, L.Z. Liang, J. Li, L. Yu, A calculation model of beam angular divergence for EAST neutral beam injector. J. Fusion Energ. **30**, 94 (2011)
10. L. Yu, C.D. Hu, S. Liu, Y.J. Xu, Water flow calorimetry system of EAST neutral beam injector. J. Fusion Energ. **32**, 547 (2013)